New Insights into Xantphos/Pd-Catalyzed C−N Bond Forming Reactions: A Structural and Kinetic Study

Liane M. Klingensmith, Eric R. Strieter, Timothy E. Barder, and Stephen L. Buchwald*

Department of Chemistry, Massachusetts Institute of Technology, Cambridge, Massachusetts 02139

Received August 18, 2005

Both (Xantphos)Pd(dba) and Pd(Xantphos)$_2$ were identified in mixtures of Pd$_2$(dba)$_3$ and Xantphos by use of ^{31}P NMR and independent syntheses. At high ligand concentrations, Pd(Xantphos)$_2$ was found to be the predominant species. Reaction calorimetry was employed to determine whether the formation of Pd(Xantphos)$_2$ affects the rate at which the Pd-catalyzed C−N bond formation occurs between 4-*tert*-butylbromobenzene and morpholine. Indeed, the concentration of Xantphos dramatically influences the activity of the catalyst, with high concentrations of Xantphos inhibiting the reaction rate due to the formation of Pd(Xantphos)$_2$. Two plausible hypotheses for the low activity of Pd(Xantphos)$_2$ as a precatalyst are (1) a slow rate of Xantphos dissociation from Pd(Xantphos)$_2$ inhibits the formation of an active (Xantphos)Pd^0 species and (2) the high degree of insolubility of Pd(Xantphos)$_2$ results in the precipitation of a significant fraction of the precatalyst from the reaction mixture. Although the equilibrium constant for ligand dissociation could not be determined by either magnetization transfer or variable-temperature experiments due to its slow rate, the more soluble Pd(4,7-di-*tert*-butylXantphos)$_2$ complex demonstrated different activity relative to Pd(Xantphos)$_2$. A comprehensive study of these two complexes indicates that the lower activity of the bis-ligated Pd species is a result of a combination of aforementioned processes, i.e., the slow rate of ligand dissociation and the insolubility of Pd(Xantphos)$_2$, with the rate of ligand dissociation serving as the primary turnover-limiting factor.

Introduction

Palladium-catalyzed C−N bond forming reactions have become one of the most important cross-coupling reactions in synthetic organic chemistry. Recently, advances have been made with the development of catalyst systems that exhibit increased selectivity and wide substrate scope.[1] One catalyst system, based on the ligand Xantphos[2] (Figure 1), has been particularly successful in broadening the substrate scope of amination reactions.[3] By utilizing a Pd/Xantphos catalyst system, difficult reactions such as the *N*-arylation of heteroarylamines and amides,[3e−g,5c] the coupling of amines with *ortho*-functionalized base-sensitive aryl halides,[4] the amination of aryl nonaflates,[3i] and the *N*-arylation of 2-oxazolidinones[3j] can be accomplished.

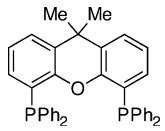

Figure 1. Xantphos (**1**).

Although Pd/Xantphos catalyst systems have been employed in various types of reactions, the reason behind their efficiency is largely unknown.[5] Van Leeuwen and co-workers initially employed Xantphos in Pd-catalyzed amination reactions[3a] after the observation that other large bite-angle ligands such as DPEphos[6] could function as excellent supporting ligands for Pd. Both Van Leeuwen[5b] and our group[5c] have demonstrated that Xantphos can serve as a *trans*-chelating ligand when bound to Pd(II). The bite-angle of Xantphos in these complexes is around 153°, which is much larger than the calculated flexible bite-angle (97−135°).[7] The cause of this large bite-angle may be the interaction between the oxygen atom on the Xantphos ligand and palladium center, which is present in the crystal structure of a oxidative addition product, i.e., (Xantphos)Pd(Ar)Br (where Ar = 4-cyanophenyl) complex.[3f] Additionally, it is possible that the Pd−O interaction facilitates key steps in the catalytic process by promoting the dissociation of one phosphine moiety of Xantphos from the metal center. More specifically, reductive elimination from a *trans*-chelating complex must be preceded by a *trans* to *cis* isomerization, an event

(1) For two recent reviews see: (a) Jiang, L.; Buchwald, S. L. *Metal-Catalyzed Cross-Coupling Reactions*, 2nd ed.; Wiley-Interscience: Weinheim. (b) Hartwig, J. F. *Handbook of Organopalladium Chemistry for Organic Synthesis*; Negishi, E., Ed.; Wiley-Interscience: Weinheim, 2002.

(2) Kranenburg, M.; van der Burgt, Y. E. M.; Kamer, P. C. J.; van Leeuwen, P. W. N. M. *Organometallics* **1995**, *14*, 3081.

(3) (a) Guari, Y.; van Es, D. S.; Reek, J. N. H.; Kamer, P. C. J.; van Leeuwen, P. W. N. M. *Tetrahedron Lett.* **1999**, *40*, 3789. (b) Harris, M. C.; Geis, O.; Buchwald, S. L. *J. Org. Chem.* **1999**, *64*, 6019. (c) Yang, B. H.; Buchwald, S. L. *Org. Lett.* **1999**, *1*, 35. (d) Wagaw, S.; Yang, B. H.; Buchwald, S. L. *J. Am. Chem. Soc.* **1999**, *121*, 10251. (e) Yin, J.; Buchwald, S. L. *Org. Lett.* **2000**, *2*, 1101. (f) Yin, J.; Buchwald, S. L. *J. Am. Chem. Soc.* **2002**, *124*, 6043. (g) Yin, J.; Zhao, M. M.; Huffman, M. A.; McNamara, J. M. *Org. Lett.* **2002**, *4*, 3481. (h) Ji, J.; Li, T.; Bunnelle, W. H. *Org. Lett.* **2003**, *5*, 4611. (i) Anderson, K. A.; Menez-Perez, M.; Priego, J.; Buchwald, S. L. *J. Org. Chem.* **2003**, *68*, 9563. (j) Cacchi, S.; Fabrizi, G.; Goggiamani, A.; Zappia, G. *Org. Lett.* **2001**, *3*, 2539. (k) Artamkina, G. A.; Sergeev, A. G.; Beletskaya, I. P. *Tetrahedron Lett.* **2001**, *42*, 4381. (l) Sergeev, A. G.; Artamkina, G. A.; Beletskaya, I. P. *Tetrahedron Lett.* **2003**, *44*, 4719. (m) Browning, R. G.; Mahmud, H.; Badarinarayana, V.; Lovely, C. J. *Tetrahedron Lett.* **2001**, *42*, 7155. (n) Anbazhagan, M.; Stephens, C. E.; Boykin, D. W. *Tetrahedron Lett.* **2002**, *43*, 4221. (o) Jean, L.; Rouden, J.; Maddaluno, J.; Lasne, M.-C. *J. Org. Chem.* **2004**, *69*, 8893.

(4) Anderson, K. A.; Buchwald, S. L. Unpublished results.

(5) For Xantphos studies see: (a) Guari, Y.; van Strijdonck, G. P. F.; Boele, M. D. K.; Reek, J. N. H.; Kamer, P. C. J.; van Leeuwen, P. W. N. M. *Chem. Eur. J.* **2001**, *7*, 475. (b) Kamer, P. C. J.; Van Leeuwen, P. W. N. M.; Reek, J. N. H. *Acc. Chem. Res.* **2001**, *34*, 895. (c) Yin, J.; Buchwald, S. L. *J. Am. Chem. Soc.* **2002**, *124*, 6043.

(6) Sadighi, J. P.; Harris, M. C.; Buchwald, S. L. *Tetrahedron Lett.* **1998**, *39*, 5327.

(7) Van der Veen, L. A.; Keeven, P. K.; Schoemaker, G. C.; Reek, J. N. H.; Kamer, P. C. J.; van Leeuwen, P. W. N. M.; Lutz, M.; Spek, A. L. *Organometallics* **2000**, *19*, 872.

10.1021/om050715g CCC: $33.50
Publication on Web 12/08/2005

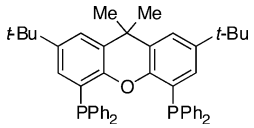

Figure 2. 4,7-Di-*tert*-butylXantphos (**2**).

that may occur through dissociation of one phosphine group of the ligand. [5b]

Van Leeuwen and co-workers have performed a detailed kinetic analysis of these reactions employing both a (Xantphos)-Pd(Ar)Br complex and a cationic (Xantphos)Pd(Ar)OTf complex.[5a] However, these studies, which are based only on initial rates, may not capture the entire kinetic picture of the reaction, as recent studies have shown anomalous rate behavior while measuring reaction kinetics under these conditions.[8a]

Our goal was to obtain insight into the composition of the catalyst based upon Xantphos and Pd in C−N bond forming reactions. These findings not only would yield important mechanistic insight but would also be advantageous in designing new ligands that could induce better selectivity and substrate scope than is currently possible. To accomplish this goal, the more soluble 4,7-di-*tert*-butylXantphos (**2**) (Figure 2)[9] was used in NMR studies and in separate syntheses of possible precatalytic species to aid in the identification of in-situ-generated precatalytic species. Both (4,7-di-*tert*-butylXantphos)Pd(dba) and Pd(4,7-di-*tert*-butylXantphos)$_2$ were identified as precatalytic species when mixtures of $Pd_2(dba)_3$ and 4,7-di-*tert*-butylXantphos were analyzed by ^{31}P NMR. The relative reactivity of the two precatalysts follows the order (4,7-di-*tert*-butylXantphos)-Pd(dba) ≫ Pd(4,7-di-*tert*-butylXantphos)$_2$ based on ^{31}P NMR studies of the coupling of 4-*tert*-butylbromobenzene and morpholine using the Pd/4,7-di-*tert*-butylXantphos system. Reaction calorimetry was also used to explore the rate of the palladium-catalyzed coupling of 4-*tert*-butylbromobenzene and morpholine using the ligand Xantphos at varying palladium-to-ligand ratios. The activity of the catalyst is dramatically dependent on the concentration of ligand relative to palladium due to formation of the much less reactive Pd(Xantphos)$_2$ species. Magnetization transfer experiments were used to probe the hypothesis that the bis-ligated Pd species has low reactivity due to a large binding constant for ligand on the bis-ligated species, and reaction calorimetry was performed using Pd(Xantphos)$_2$ and Pd(4,7-di-*tert*-butylXantphos)$_2$ as precatalysts to identify whether the solubility of the bis-ligated species affects reaction rate. It was discovered that the main cause for the low reactivity of Pd-(Xantphos)$_2$ is a large binding constant for Xantphos from the bis-ligated species, causing the generation of the active (Xantphos)Pd^0 species to be relatively slow. Additionally, the insoluble nature of Pd(Xantphos)$_2$ in THF and toluene is apparent by examining the differences in reactivity between Pd-(Xantphos)$_2$ and Pd(4,7-di-*tert*-butylXantphos)$_2$.

Results and Discussion

Initial studies focused on determining the structure(s) of the Xantphos/Pd precatalyst. We wanted to ascertain the nature and distribution of species present in a mixture of Xantphos and $Pd_2(dba)_3$ by ^{31}P NMR. However, due to the low solubility of Xantphos and $Pd_2(dba)_3$ in common organic solvents, experiments utilizing standard NMR techniques could not be conducted. To circumvent this issue, initial studies were conducted using the more soluble 4,7-di-*tert*-butylXantphos, **2**. The ^{31}P NMR spectrum of a mixture of $Pd_2(dba)_3$ and 4,7-di-*tert*-butylXantphos in a 1:1 L:Pd ratio exhibits two separate resonances, corresponding to two distinct species (Figure 3). The ^{31}P NMR spectrum of complex **B** has an intricate splitting pattern at low temperature that begins to coalesce to one peak

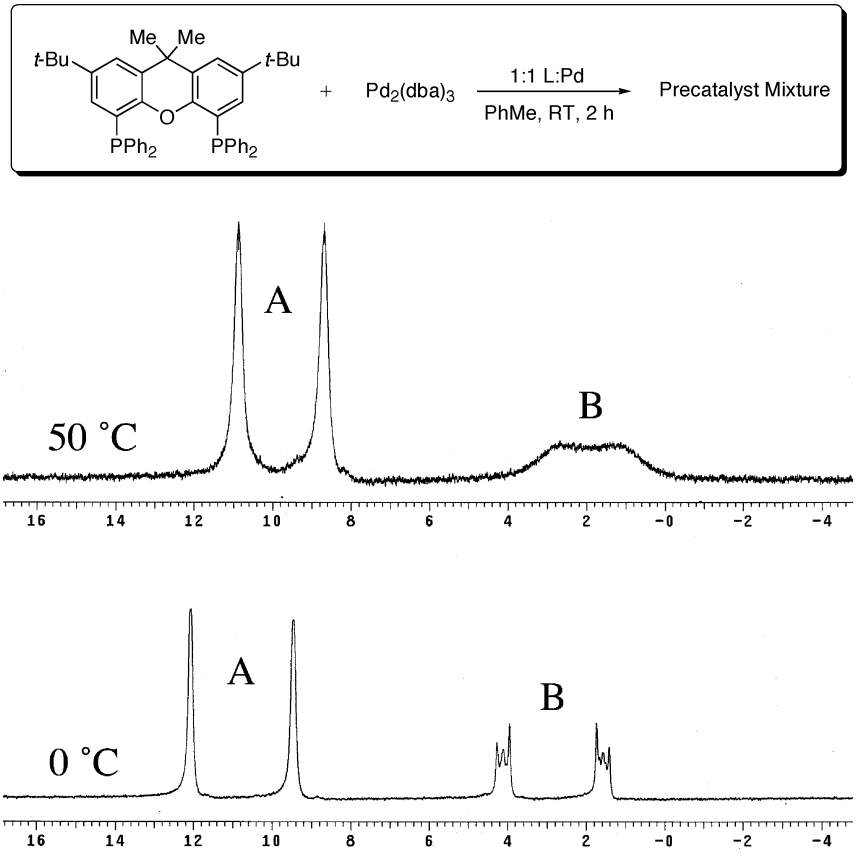

Figure 3. ^{31}P NMR spectra of the precatalyst mixture (1:1 Pd:L) at 0 and 50 °C.

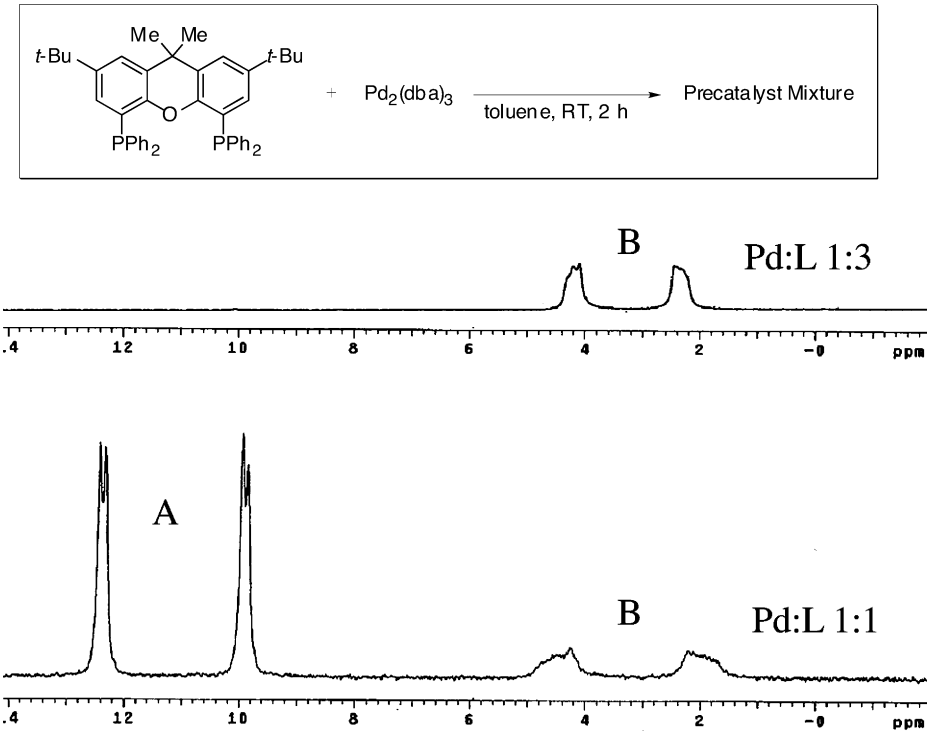

Figure 4. ^{31}P NMR spectra of the precatalyst mixture (1:1 and 1:3 Pd:L) at RT.

Scheme 1. Synthesis of Various (4,7-Di-*tert*-butylXantphos)Pd Complexes

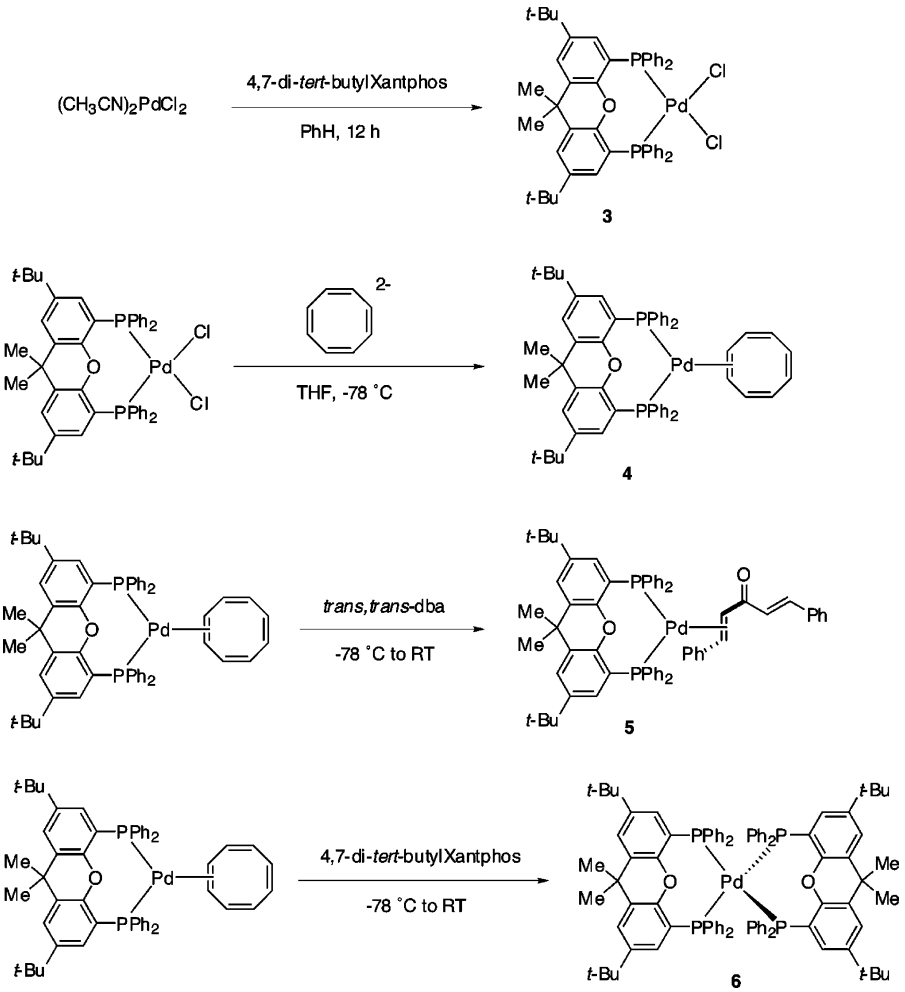

at higher temperatures. The other resonances, ascribed to complex **A**, are consistent with two inequivalent phosphorus atoms bound to one palladium center. The ^{31}P NMR spectrum of a mixture similar to that above, but with an excess of **2** (i.e.,

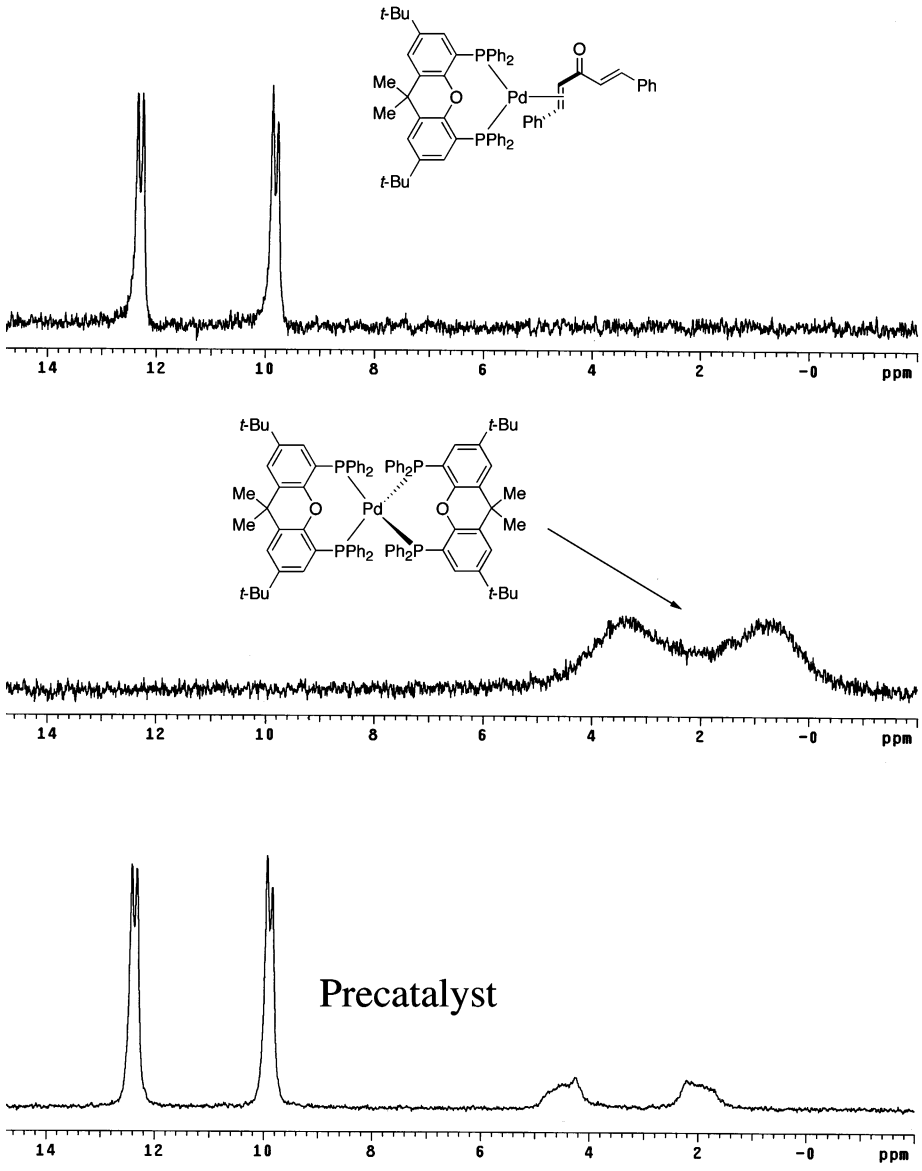

Figure 5. ^{31}P NMR spectra of palladium complexes derived from (4,7-di-*tert*-butylXantphos)Pd(COT). The spectra of Pd(4,7-di-*tert*-butylXantphos)$_2$ and (4,7-di-*tert*-butylXantphos)Pd(dba) were obtained in THF-d_8, while the spectrum of the precatalyst mixture was obtained in PhMe-d_8.

3:1 L:Pd), indicated the presence of only one species, aside from unbound ligand, that corresponds to complex **B** (Figure 4). This is suggestive of the conversion of complex **A** into complex **B** at high ligand concentrations. The same experiment was attempted with Xantphos; however, an insoluble yellow-green precipitate formed, rendering a solution state NMR analysis impossible. Fortunately, Pd(Xantphos)$_2$ could be isolated from a mixture of Xantphos and $Pd_2(dba)_3$ as a yellow solid[10] and was characterized by both MALDI-TOF-MS and elemental analysis.

To identify the resonances observed in the ^{31}P NMR of the precatalyst mixture, complexes **3**, **5**, and **6** were independently prepared (Scheme 1). (4,7-Di-*tert*-butylXantphos)$PdCl_2$ (**3**) was synthesized using a procedure analogous to that used in the preparation of $PdCl_2$(dppf).[11] By utilizing the straightforward route to bisphosphine-cyclooctatetraene Pd(0) complexes developed by Brown and Cooley,[12] **4** was assembled from **3**. As cyclooctatetraene is an extremely labile ligand, both (4,7-di-*tert*-butylXantphos)Pd(dba)[13] (**5**) and Pd(4,7-di-*tert*-butylXantphos)$_2$ (**6**) can be easily obtained from **3**; the ^{31}P NMR spectra are illustrated in Figure 5. (4,7-Di-*tert*-butylXantphos)Pd(dba) corresponds to the resonances at 9.8 and 12.4 ppm. The two phosphorus atoms on palladium are inequivalent due to the nonsymmetric bonding of dba ligand on the palladium center, which accounts for the observed P−P coupling. The ^{31}P NMR resonances for the phosphorus atoms in Pd(*tert*-butylXantphos)$_2$ appear at 0.8 and 3.4 ppm (in THF). As illustrated in Figure 4,

(8) (a) Singh, U. K.; Strieter, E. R.; Blackmond, D. G.; Buchwald, S. L. *J. Am. Chem. Soc*. **2002**, *124*, 14104. (b) Nielsen, L. P. C.; Stevenson, C. P.; Blackmond, D. G.; Jacobsen, E. N. *J. Am. Chem. Soc*. **2004**, *126*, 1360. (c) Streiter, E. R.; Blackmond, D. G.; Buchwald, S. L. *J. Am. Chem. Soc*. **2005**, *127*, 4120.

(9) van der Veen, L. A.; Kamer, P. C. J.; van Leeuwen, P. W. N. M. *Angew. Chem., Int. Ed*. **1999**, *38*, 336.

(10) Once isolated, Pd(Xantphos)$_2$ appears green if there is a small amount of palladium black present.

(11) Hayashi, T.; Konishi, M.; Kobori, Y.; Kumada, M.; Higuchi, T.; Hirotsu, K. *J. Am. Chem. Soc*. **1984**, *106*, 158.

(12) (a) Brown, J. M.; Cooley, N. A. *Organometallics* **1990**, *9*, 353. (b) Katz, T. J.; Garratt, P. J. *J. Am. Chem. Soc.* **1964**, *86*, 4876.

(13) This is most likely the complex formed; however, attempts to isolate and purify this complex have not been successful.

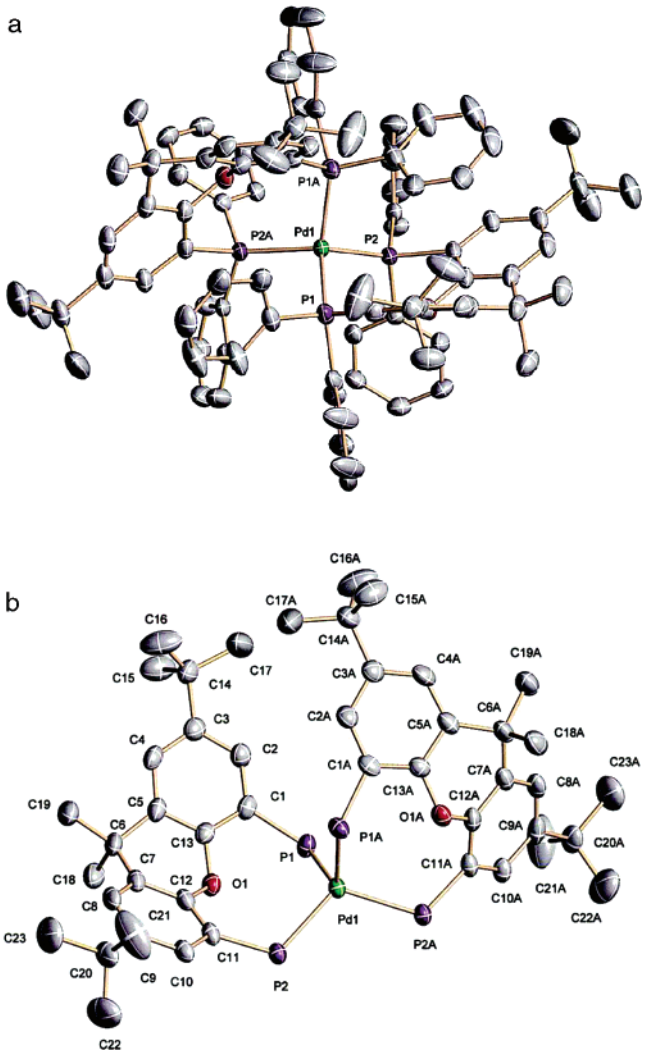

Figure 6. (a) ORTEP diagram of Pd(4,7-di-*tert*-butylXantPhos)$_2$ with hydrogen atoms, benzene molecule, and ether molecule removed for clarity. Thermal ellipsoids are at 30% probability. (b) ORTEP diagram of Pd(4,7-di-*tert*-butylXantPhos)$_2$ with hydrogens, phenyl groups, benzene molecule, and ether molecule removed for clarity. Thermal ellipsoids are at 30% probability.

the ^{31}P NMR spectrum of this complex at 0 °C possesses a complex splitting pattern, suggesting that **6** does not possess tetrahedral geometry.

An X-ray-quality crystal of **6**[14] was grown by preparing the complex by the route shown in Scheme 1 and subsequently layering a solution of **6** in benzene with ether. The ORTEP diagram is shown in Figure 6a. To allow for better interpretation, the phenyl groups have been removed for clarity, as shown in Figure 6b. The asymmetric unit contains a molecule of Pd(4,7-di-*tert*-butylXantphos)$_2$ with slightly distorted tetrahedral geometry (Pd−P bond distances and angles in Table 1) as well as a half-molecule of Pd(*tert*-butylXantphos)$_2$ possessing C_2 symmetry. It is apparent from both solution state NMR studies, conducted at RT and 60 °C, and X-ray crystallography, conducted at −173 °C, that this complex is fluxional in both states likely due to the crowding around the Pd center (Figure 7). The distortions from a tetrahedral geometry most likely exist due to the highly crowded and geometrically strained Pd center constantly attempting to reside in a minimum energy structure.

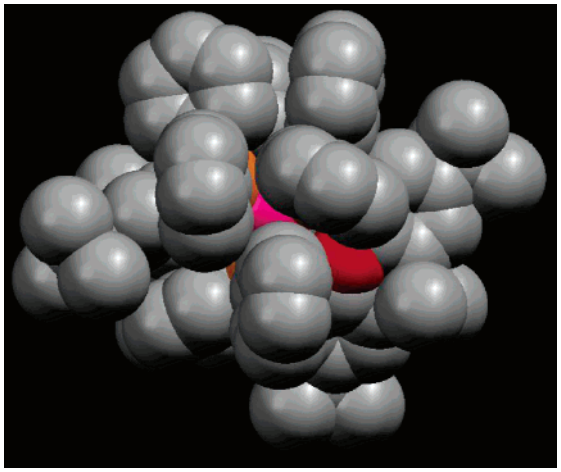

Figure 7. Space-filling model of Pd(4,7-di-*tert*-butylXantphos)$_2$. Gray = carbon, red = oxygen, orange = phosphorus, and pink = palladium.

Table 1. Selected Bond Lengths (Å) and Bond Angles (deg) for Pd(4,7-di-*tert*-butylXantphos)$_2$

bond	length	bond	angle
Pd(1)−P(1)	2.3884(12)	P(1)−Pd(1)−P(2)	108.73(4)
Pd(1)−P(2)	2.3454(11)	P(1)−Pd(1)−P(1A)	106.49(4)
Pd(2)−P(3)	2.3857(11)	P(3)−Pd(2)−P(4)	108.79(4)
Pd(2)−P(4)	2.3798(11)	P(3)−Pd(2)−P(5)	113.47(4)
Pd(2)−P(5)	2.3870(10)	P(3)−Pd(2)−P(6)	108.94(4)
Pd(2)−P(6)	2.3998(12)	P(4)−Pd(2)−P(5)	108.08(4)
		P(4)−Pd(2)−P(6)	108.05(4)
		P(5)−Pd(2)−P(6)	109.38(4)

To test the relative reactivity of (4,7-di-*tert*-butylXantphos)-Pd(dba) and Pd(*tert*-butylXantphos)$_2$ in an amination reaction, a slurry of NaO*t*-Am, morpholine, and 4-*tert*-butylbromobenzene was injected into a NMR tube, sealed with a Teflon septum, containing a precatalyst mixture as prepared above. The NMR tube was quickly placed in the spectrometer preheated to 60 °C. It was found that Pd(*tert*-butylXantphos)$_2$ remains unchanged, while a large quantity of (4,7-di-*tert*-butylXantphos)-Pd(dba) is converted into other unidentified species.[15] Presumably, these species stem from amine and/or NaO*t*-Am addition to the dibenzylideneacetone ligand bound to the Pd center. Importantly, these data suggest that Pd(*tert*-butylXantphos)$_2$ is relatively unreactive compared to (4,7-di-*tert*-butylXantphos)-Pd(dba).

Reaction calorimetry experiments were conducted to verify that the rate of reaction was affected by the ratio of (Xantphos)-Pd(dba) to Pd(Xantphos)$_2$ in the precatalyst mixture. The palladium-catalyzed coupling of 4-*tert*-butylbromobenzene and morpholine at 60 °C (Figure 8) was used in this investigation due to its rapid reaction rate and high conversion of aryl bromide to product.[16] Our initial studies revealed that the Pd:Xantphos ratio has a dramatic effect on reaction rate, as shown in Figure 8. Interestingly, the initial addition of Xantphos increases the rate of C−N bond formation; however, at higher Xantphos concentrations the reaction rate is suppressed. Ultimately, a Xantphos:Pd ratio of 1:1 is optimal for maximum turnover frequency, suggesting that the active catalyst contains only one

(14) The only other palladium(0) bis-xanthene crystal structure reported is Pd(ethylXantphos)$_2$ (in this case, it is diethylphosphines instead of diphenylphosphines on the xanthene backbone): Raebiger, J. W.; Miedaner, A.; Curtis, C. J.; Miller, S. M.; Anderson, O. P.; DuBois, D. L. *J. Am. Chem. Soc.* **2004**, *126*, 5502.

(15) See Supporting Information for NMR spectra.

(16) Toluene was used to make a stock solution of Xantphos so that a more accurate amount of Xantphos could be injected into the reaction vessel. Toluene was used rather than 1,4-dioxane due to solubility problems.

Scheme 2. Equilibria of Palladium/Xantphos Species

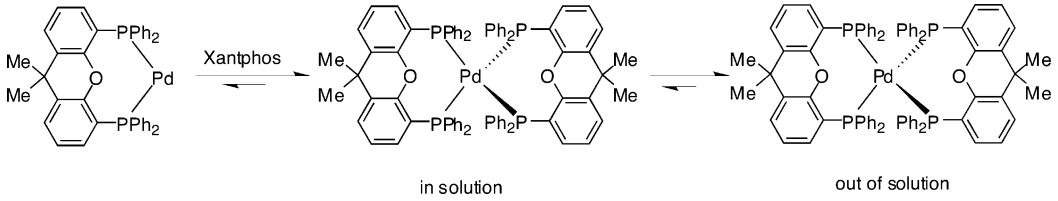

Xantphos ligand. Indeed, both Sigman and Stahl have recently observed similar behavior while examining the rate dependence on ligand concentration during the palladium-catalyzed aerobic oxidation of alcohols.[17] Thus, on the basis of both the ^{31}P NMR and calorimetric experiments, it is believed that at higher concentrations of Xantphos formation of Pd(Xantphos)$_2$ occurs, which dominates the Pd speciation, thereby leading to a decrease in the reaction rate. Others have reported trends that can account for the formation of this species during Pd-catalyzed C−N bond forming processes. For example, our group has reported that "an unusual dependence on catalyst loading", where the reactions being studied were more efficient at lower catalyst concentrations, was observed.[5c] Moreover, Yin has reported that difficult reactions employing Xantphos are often run at low concentrations (0.25−0.13 M), which would minimize the formation of Pd(Xantphos)$_2$.[3g]

There exist as least two possible hypotheses that could account for the low activity of Pd(Xantphos)$_2$ in Pd-catalyzed C−N bond forming reactions. The first premise is that an equilibrium process exists between the bis-ligated palladium species and the mono-ligated palladium species in solution, and this equilibrium favors the bis-ligated species (Scheme 2). The second possibility is that a solubility equilibrium process exists that favors the unsolvated Pd(Xantphos)$_2$ and therefore causes the majority of the Pd to reside as a highly insoluble precipitate, unable to enter the catalytic cycle.

Attempts were made using a ^{31}P NMR magnetization transfer experiment to measure the rate of dissociation of a ligand from Pd(Xantphos)$_2$, similar to a procedure that has been previously reported by Grubbs and co-workers.[18] A solution containing Pd(4,7-di-*tert*-butylXantphos)$_2$ and 4,7-di-*tert*-butylXantphos (1.0:1.5) in benzene-d_6 was allowed to reach equilibrium in an NMR probe. Once this occurred, the resonance corresponding to the free ligand was selectively inverted by a 180° pulse. After variable mixing times between 0.01 and 5.12 s, a nonselective 90° pulse was applied. Using this method, if free ligand were to exchange rapidly with ligand bound to the Pd center, the peak area for the complex would decrease following exchange with the inverted signal of the free ligand. However, even at 60 °C no change in the value of the peak area was observed, implying no appreciable exchange (or less exchange than is capable of being detected by NMR) was occurring between the complexed and free ligand. This method is useful only for rates of exchange that are large enough relative to (1) the relaxation rate of the complexed ligand and (2) the relaxation rate of the free ligand. That is, the rate of magnetization loss due to exchange of the complexed ligand with free ligand must be large relative to the rate at which the NMR signal of the complexed ligand returns to equilibrium and/or the rate at which the free ligand relaxes back to equilibrium following selective inversion. We found that in this case exchange is too slow to measure before relaxation occurs, thus preventing the quantification of the dissociation constant. These data suggest that the binding constant of **2** is very large in Pd(4,7-di-*tert*-butylXantphos)$_2$, which is consistent with its poor activity as a precatalyst.

To test the hypothesis that the insolubility of Pd(Xantphos)$_2$ restricts its activity as a precatalyst, experiments were performed at varying ligand-to-palladium ratios with both Xantphos and 4,7-di-*tert*-butylXantphos (Figure 9). At high ligand-to-palladium ratios (>1.6), the catalyst based upon **2** continues to promote the reaction. However, performing the reaction under identical conditions, except for substitution of Xantphos for 4,7-di-*tert*-butylXantphos, did not yield product, due to the formation of the inactive Pd(Xantphos)$_2$ species. However, at L:Pd ratios between 1 and 1.6, the kinetic rate profiles are essentially identical for Xantphos and 4,7-di-*tert*-butylXantphos.

To further examine the hypothesis that the insolubility of Pd(Xantphos)$_2$ can restrict its activity as a precatalyst, reactions were catalyzed by employing both Pd(Xantphos)$_2$ and Pd(*tert*-butylXantphos)$_2$ as precatalysts. Rate versus time plots are depicted in Figure 10a, and a plot of rate versus fractional conversion is depicted in Figure 10b for the coupling of 4-*tert*-butylbromobenzene and morpholine.

The reaction catalyzed by Pd(Xantphos)$_2$ exhibits a very interesting kinetic profile in that the rate is slowly increasing throughout the reaction. This is in contrast to the kinetic profile of the corresponding reaction with Pd(4,7-di-*tert*-butylXantphos)$_2$, where the rate is relatively constant throughout the reaction, corresponding to zero-order kinetics. These kinetic data are very similar to an observation of zero-order kinetics made

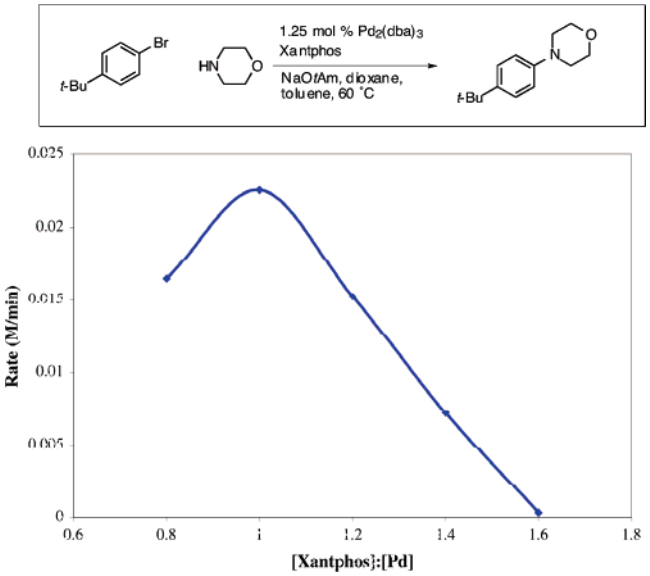

Figure 8. Reaction rate vs [Xantphos]:[Pd] ratio. [ArBr]$_0$ = 0.25 M; [Amine]$_0$ = 0.30 M (1.2 equiv); [NaO*t*Am]$_0$ = 0.35 M (1.4 equiv); $Pd_2(dba)_3$ 2.5 mol % Pd based on ArBr; Xantphos 2−4 mol % based on ArBr; 3 mL of 1,4-dioxane and 1 mL of toluene. Reaction rate is at 10% conversion of ArBr.

(17) (a) Schultz, M. J.; Adler, R. S.; Zierkiewicz, W.; Privalov, T.; Sigman, M. S. *J. Am. Chem. Soc.* **2005**, *127*, 8499. (b) Steinhoff, B. A.; Guzei, I. A.; Stahl, S. S. *J. Am. Chem. Soc.* **2004**, *126*, 11268. (c) Steinhoff, B. A.; Stahl, S. S. *Org. Lett.* **2002**, *4*, 4179.

(18) Sanford, M. S.; Love, Jennifer, A.; Grubbs, R. H. *J. Am. Chem. Soc.* **2001**, *123*, 6543.

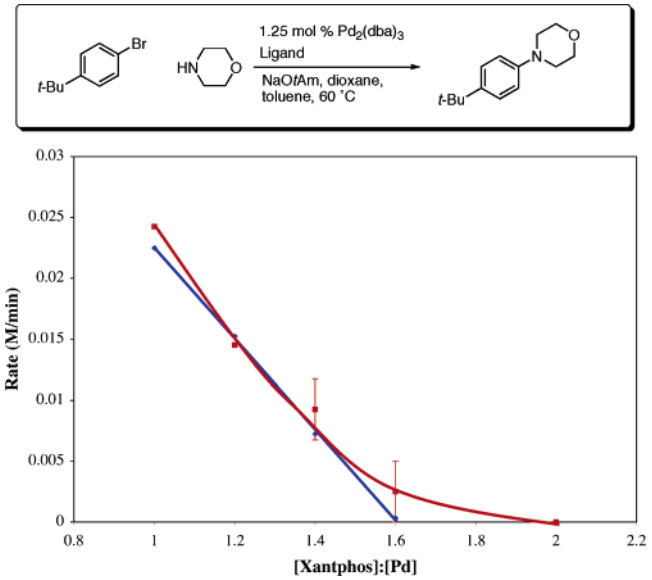

Figure 9. Plot of rate vs [Ligand]:[Pd] for both Xantphos (blue line) and 4,7-di-*tert*-butylXantphos (red line). $[ArBr]_0 = 0.25$ M; $[Amine]_0 = 0.30$ M (1.2 equiv); $[NaOtAm]_0 = 0.35$ M (1.4 equiv); $Pd_2(dba)_3$ 2.5 mol % Pd based on ArBr; ligand 2.0−4.0 mol % based on ArBr; 3 mL of 1,4-dioxane and 1 mL of toluene.

both by van Leeuwen[5a] and by Hartwig[19] while studying palladium-catalyzed C−N bond formation using a Pd/Xantphos and a Pd/BINAP catalyst system, respectively. Blackmond and Buchwald[8a] later demonstrated that the zero-order dependence on substrate may arise from the slow rate of active catalyst formation. This would be the case if a slow dissociation of **2** from Pd(4,7-di-*tert*-butylXantphos)$_2$ was occurring. A slow dissociation process is also occurring from Pd(Xantphos)$_2$ in addition to a slow equilibrium allowing more precatalyst into solution, a process that accounts for the increasing rate of reaction.

Conclusions

Products from mixing Xantphos and $Pd_2(dba)_3$ were identified as Pd(Xantphos)$_2$ and (Xantphos)Pd(dba). This was accomplished by separately synthesizing the analogous 4,7-di-*tert*-butylXantphos species and comparing ^{31}P NMR spectra. (Xantphos)Pd(dba) serves as the precatalyst, and Pd(Xantphos)$_2$ demonstrates extremely low activity as a precatalyst.

Reaction rates were essentially identical for reactions catalyzed by Xantphos and 4,7-di-*tert*-butylXantphos at L:Pd ratios between 1.0 and 1.5, suggesting that the insolubility of Pd(Xantphos)$_2$ is not the cause of its low activity, since Pd(*tert*-butylXantphos)$_2$ is entirely soluble. Furthermore, it was demonstrated through reaction calorimetry that Pd(Xantphos)$_2$ is in equilibrium with Pd(Xantphos) by use of Pd(Xantphos)$_2$ as the precatalyst. This equilibrium was probed by use of a magnetization transfer experiment, and it was found that formation of Pd(Xantphos)$_2$ in the palladium-catalyzed amination of 4-*tert*-butylbromobenzene significantly decreases the rate of reaction, not due to solubility, but due to a very large binding constant for the ligand on the bis-ligated species, which causes a slow generation of mono-ligated active catalyst. This is the first time the equilibrium of phosphine dissociation from a bis(xanthane-based phosphine)Pd(0) complex has been examined and subsequently applied to determining the detrimental effect of using a ratio of ≥ 1.5:1 L:Pd, where L = Xantphos, in C−N bond forming reactions.

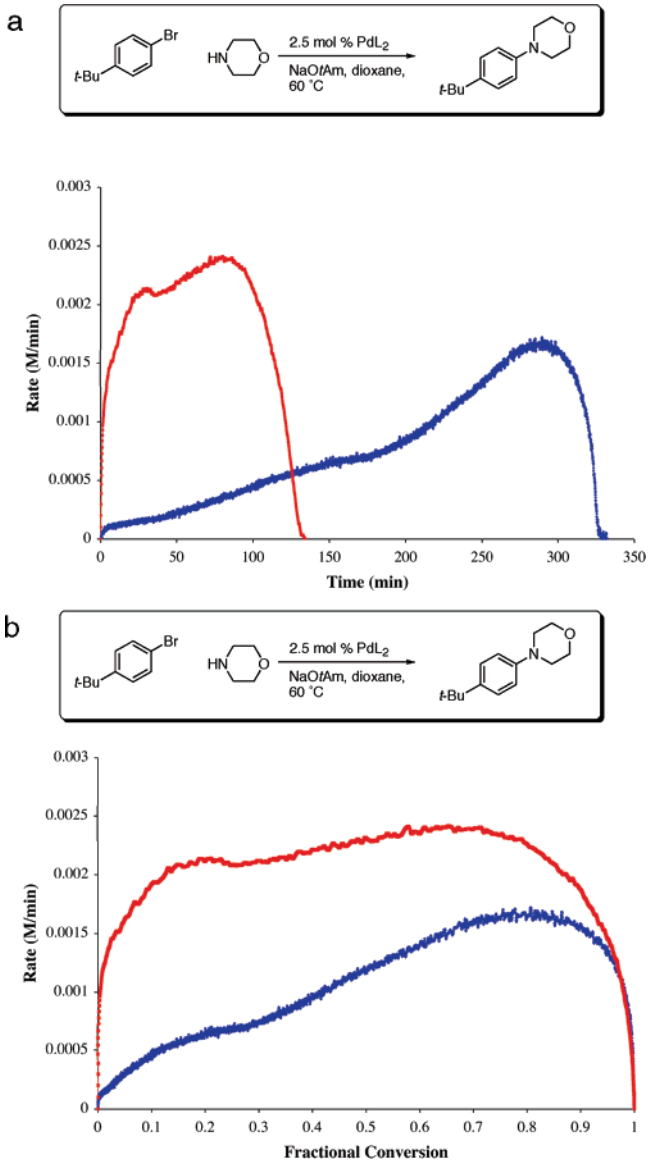

Figure 10. (a) Reaction rate vs time for reactions catalyzed by Pd(4,7-di-*tert*-butylXantphos)$_2$ (red line) and Pd(Xantphos)$_2$ (blue line). $[ArBr]_0 = 0.25$ M; $[Amine]_0 = 0.30$ M (1.2 equiv); $[NaOtAm]_0 = 0.35$ M (1.4 equiv); 2.5% Pd(L)$_2$ based on [ArBr]; 4 mL of 1,4-dioxane. (b) Reaction rate vs fractional conversion for reactions catalyzed by Pd(4,7-di-*tert*-butylXantphos)$_2$ (red line) and Pd(Xantphos)$_2$ (blue line). $[ArBr]_0 = 0.25$ M; $[Amine]_0 = 0.30$ M (1.2 equiv); $[NaOtAm]_0 = 0.35$ M (1.4 equiv); 2.5% Pd(L)$_2$ based on [ArBr]; 4 mL of 1,4-dioxane. $\Delta H_{rxn} = 203.6$ kJ/mol for Pd(4,7-di-*tert*-butylXantphos)$_2$ and $\Delta H_{rxn} = 214.1$ kJ/mol for Pd(Xantphos)$_2$.

Materials and Methods

Reagents. Toluene and THF were purchased from J. T. Baker in CYCLE-TAINER solvent delivery kegs and vigorously purged with argon for 2 h. The solvent was further purified by passing it under argon pressure through two packed columns of neutral alumina (THF) or through neutral alumina and copper(II) oxide (toluene). 1,4-Dioxane, benzene, and morpholine were purchased from Aldrich Chemical Co. in SureSeal containers and taken into a glovebox before use. Xantphos, dichlorobis(acetonitrile)palladium(II), tris(dibenzylideneacetone)dipalladium(0), and lithium granules

(19) Alcazar-Roman, L. M.; Hartwig, J. F.; Rheingold, A. L.; Liable-Sands, L. M.; Guzei, I. A. *J. Am. Chem. Soc.* **2000**, *122*, 4618.

were acquired from Strem Chemicals, Inc. and used without further purification. 1-Bromo-4-*tert*-butylbenzene was purchased from Aldrich Chemical Co. and distilled from CaH_2 prior to use. Sodium *tert*-amylate (NaO*t*Am), purchased from Aldrich, was stored and used inside of the glovebox. 4,5-Dibromo-2,7-di-*tert*-butyl-9,9-dimethylxanthene, *n*-BuLi (2.5 M in SureSeal bottle), and cyclooctatetraene were purchased from Aldrich Chemical Co. and used without further purification. Chlorodiphenylphosphine (98%) was purchased from Strem Chemical Co. and distilled over CaH_2 under reduced pressure prior to use. All reagents used in reaction calorimetry experiments were handled and stored in a nitrogen-filled glovebox, except for tris(dibenzylideneacetone)dipalladium-(0), which was weighed in air into a septum-sealed vial. This vial was then evacuated/backfilled with argon three times before it was taken into a glovebox.

Analytical Methods. ^{1}H NMR spectra were obtained on either a Bruker 400 MHz or a Varian Mercury 300 MHz spectrometer, with chemical shifts reported with respect to residual solvent peaks. ^{31}P{^{1}H} NMR spectra were obtained on either a Varian 500 MHz or a Varian Mercury 300 MHz, with chemical shifts reported with respect to calibration with an external standard of phosphoric acid (0 ppm). MALDI-TOF was performed on a Bruker Omniflex calibrating externally with a ProteoMass Peptide MALDI-MS calibration kit. Melting points (uncorrected) were obtained on a Mel-Temp capillary melting point apparatus. Gas chromatographic analyses were performed on a Hewlett-Packard 6890 gas chromatography instrument with an FID detector using a 25 m × 0.20 mm capillary column with cross-linked methyl siloxane as a stationary phase. Elemental analyses were obtained from Atlantic Microlab, Inc. (Norcross, GA).

Reaction Calorimetry Experimental Details. Reactions were performed in either an Omnical SuperCRC or an Omnical Reactmax reaction calorimeter. The instrument contains an internal magnetic stirrer and a differential scanning calorimeter (DSC), which compares the heat released or consumed in a sample vessel to an empty reference vessel. The reaction vessels were 16 mL borosilicate screw-thread vials fit with open-top black phenolic screw caps and white PTFE septa (KimbleBrand) charged with Teflon-coated magnetic stir bars. Sample volumes did not exceed 4.2 mL. A stock solution of Xantphos or *tert*-butylXantphos was made by dissolving 0.250 mmol of ligand (145 mg of Xantphos, 173 mg of *tert*-butylXantphos) in 5.0 mL of toluene in a volumetric flask to make a 0.050 M solution. $Pd_2(dba)_3$ was weighed in air and brought into the glovebox by evacuating and backfilling a small vial with argon three times. Dioxane (1 mL) was then added and stirred to form a slurry. This slurry was then added to the previously weighed NaO*t*Am in the reaction vessel. The desired amount of ligand was added by taking a portion of the stock solution and diluting to a total volume of 1.0 mL in toluene, so that each reaction contained a constant amount of toluene with varying amounts of ligand (i.e., if 0.025 mmol of ligand was desired, 0.50 mL of the stock solution was delivered to a vial and 0.50 mL of toluene was added; if 0.03 mmol of ligand was desired, 0.60 mL of the stock solution was delivered to a vial, and 0.40 mL of toluene was added). This solution of ligand was added to the calorimeter vial containing the NaO*t*Am and $Pd_2(dba)_3$, and finally 2.0 mL of dioxane was added and the reaction vessel was sealed. This vessel was then removed from the glovebox and placed in the calorimeter and stirred for 1 h, allowing the contents of the vessel to reach thermal equilibrium. Simultaneously, a syringe containing 1-bromo-4-*tert*-butylbenzene and morpholine was placed in the sample injection port of the calorimeter and was allowed to thermally equilibrate. The reaction was initiated by injecting the mixture of aryl bromide and amine into the stirred catalyst/NaO*t*Am solution. The temperature of the DSC was held constant at 333 K using the internal temperature controller in the calorimeter, ensuring that the reaction would proceed under isothermal conditions. A raw data curve was

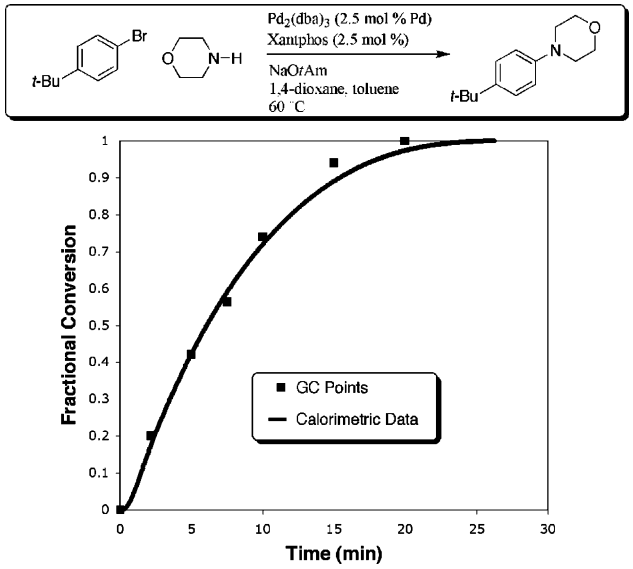

Figure 11. Fraction conversion vs time for calorimetric and GC data. $[ArBr]_0$ = 0.25 M; $[Amine]_0$ = 0.30 M (1.2 equiv); $[NaOtAm]_0$ = 0.35 M (1.4 equiv; 1:1 Xantphos:Pd from $Pd_2(dba)_3$ 2.5 mol % Pd based on ArBr; 3 mL of 1,4-dioxane and 1 mL of toluene.

produced by measuring the heat flow from the sample vessel every 6 s during the reaction. Due to the delay between the instantaneous heat flow being evolved from the reaction vessel and the time the thermophile sensor detects the heat flow, the raw data curve must be calibrated. To accomplish this calibration, a constant amount of current was passed through a resistor in the sample chamber of the calorimeter, thereby producing a known quantity of heat. This process results in a response curve, which is then transformed into a square wave, allowing for the response time of the instrument to be calculated using the WinCRC software. Application of the response time to the raw data results in a "tau-corrected data curve". The tau-corrected data curve is a plot of heat flow (mJ s^{-1}) versus time. The reaction rate, which is directly proportional to the heat flow (eq 1), fractional conversion (eq 2), and instantaneous concentrations of reactants/products can all be calculated from this tau-corrected data curve.

$$q = \Delta H_{rxn} V r \quad (1)$$

$$\text{fractional conversion} = \frac{\int_{t_0}^{t} q(t)\,dt}{\int_{t_0}^{t} q(t)\,dt} \quad (2)$$

As a control, conversion measured by GC analysis was compared to conversion measured by heat flow (Figure 11). Agreement between the two curves suggests that calorimetric analysis was a valid method for studying rates of this type of reaction.

Crystal Structure Determination of Pd(4,7-di-*tert*-butylXantphos)$_2$. Crystals suitable for X-ray diffraction were obtained by layering ether on a saturated solution of Pd(4,7-di-*tert*-butylXantPhos)$_2$ in benzene in a glovebox. A single crystal (0.17 × 0.12 × 0.09 mm^3) was mounted on a magnetic glass pin and placed on the goniometer head under a stream of N_2 delivered from a Cyrostream 700 at 100 K. A Siemens Platform three-circle diffractometer equipped with an APEX CCD detetctor was used to obtain the data. The crystal was exposed to Mo Kα radiation (λ = 0.71073 Å), collecting 10 s frames, of which 230 195 measured and 26 495 independent reflections were observed, with R_{int} = 0.1009 in *C*2/*c* (space group #15), to d = 0.80 (2θ = 52.78°). Data were processed using SAINT supplied by Siemens Industrial Automation, Inc., and structure determination was completed by

direct methods using SHELXTL, V6.10, G. M. Sheldrick, University of Göttingen. The structure was refined on F^2 by full-matrix least-squares methods, and an absorption correction was applied with SADABS. All non-hydrogen atoms were refined anistropically, except for the extremely disorded ether molecule. All hydrogens were placed in calculated positions and left to ride on their parent atoms. The benzene molecule was disordered and each carbon was set at half-occupancy. The refinement of 1465 parameters using 26 495 reflections and 0 restraints gave $R_1 = 0.0637$, $wR_2 = 0.1639$ [$I > 2\sigma(I)$], goodness of fit on $F^2 = 1.070$, $\Delta\rho_{max/min} = 1.398/-0.967$ e Å^{-3}.

Magnetization Transfer Experiment. Pd(4,7-di-*tert*-butylXantphos)$_2$ (34.2 mg, 0.0230 mmol) and 4,7-di-*tert*-butylXantphos (24.2 mg, 0.0350 mmol) were weighed inside of the glovebox into a small vial. They were dissolved in benzene-d_6 (0.70 mL) and transferred to a screw-cap septum-sealed NMR tube. The tube was equilibrated in the NMR probe at either 20 or 60 °C. The free *tert*-butylXantphos was selectively inverted using a 180° pulse. After variable mixing times between 0.0100 and 5.12 s, a nonselective 90° pulse was applied. Sixteen transients with a relaxation delay of 35 s (T_1 of Pd(4,7-di-*tert*-butylXantphos)$_2$ is 1.17 s; T_1 of 4,7-di-*tert*-butylXantphos is 6.46 s) were needed to obtain a spectrum with an acceptable signal-to-noise ratio. ^{1}H decoupling was applied during the 90° pulse. Integration values at the variable mixing times for the complex were determined and found to remain constant, meaning that no detectable exchange occurred between the complexed and free ligand.

Sample Analysis of Precatalyst by ^{31}P NMR. 4,7-Di-*tert*-butylXantphos (69.9 mg, 0.100 mmol) and $Pd_2(dba)_3$ (45.9 mg, 0.0500 mmol) were dissolved in toluene (2.0 mL) and allowed to stir for 2 h inside of a glovebox. This solution was filtered over a glass frit to remove insoluble matter and concentrated to a volume of 0.7 mL. This solution was then transferred to a septum-sealed NMR tube.

Material Preparation. Preparation of 4,7-Di-*tert*-butylXantphos (2). To a flame-dried 500 mL round-bottom flask was added 4,5-dibromo-2,7-di-*tert*-butyl-9,9-dimethylxanthene (5.0 g, 10.4 mmol), which was dissolved in THF (150 mL) under a positive flow of argon. This solution was cooled to −78 °C, and *n*-BuLi (8.8 mL of a 2.5 M solution in hexanes, 22 mmol) was added dropwise over 20 min. The solution was allowed to stir at −78 °C for 2 h, then chlorodiphenylphosphine (4.5 mL, 24 mmol) was added dropwise over 45 min. With stirring, the solution was allowed to warm to room temperature overnight. The solution was washed with water (3 × 100 mL), dried over $MgSO_4$, and concentrated with the aid of a rotary evaporator to give a light yellow oil. With vigorous stirring, EtOH (50 mL) was slowly added to the yellow oil to form a slurry of crude 4,7-di-*tert*-butylXantphos, which was filtered and recrystallized from toluene/EtOH to afford 6.13 g (85%) of a white solid. ^{1}H NMR (CD_2Cl_2, 300 MHz): δ 7.42 (d, ^4J(H,H) = 2.40 Hz, 2H), 7.24 (m, 20H), 6.55 (m, 2H), 1.67 (s, 6H), 1.11 (s, 18H). ^{31}P NMR{^{1}H} (CD_2Cl_2, 300 MHz): δ −16.3. Lit. mp 194−195 °C,[10] experimental mp 194−195 °C.

Preparation of PdCl$_2$(4,7-di-*tert*-butylXantphos) (3). This procedure was adapted from Hayashi's procedure to make $PdCl_2$(dppf).[11] A slurry of benzene (20 mL) and dichlorobis(acetonitrile)-palladium(II) (518 mg, 2.00 mmol) was allowed to stir in a septum-sealed 100 mL round-bottom flask in a glovebox. 4,7-Di-*tert*-butylXantphos (1.38 g, 2.00 mmol) was dissolved in benzene (20 mL) and added slowly with stirring to the dichlorobis(acetonitrile)-palladium(II) slurry. This mixture was allowed to stir for 12 h, during which time a yellow precipitate, as well as an orange solution, formed. The yellow solid was filtered over a glass frit in a glovebox and washed with benzene (10 mL) and ether (10 mL) until the supernatant was clear and finally dried under high vacuum to afford 457 mg (29%) of a yellow solid. Mp: 171 °C dec. IR (KBr): 3057, 2964, 2906, 2869, 1479, 1436, 1426, 1395, 1364, 1255, 1234, 1190, 1094, 741, 706, 692 cm^{-1}. ^{1}H NMR (CD_2Cl_2, 300 MHz): δ 7.70 (d, ^4J(H,H) = 1.70 Hz, 2H), 7.23 (m, 22H), 1.87 (s, 6H), 1.26 (s, 18H). ^{13}C NMR (CD_2Cl_2, 500 MHz): δ 153.3 (m), 148.4 (m), 135.7 (m), 135.0 (m), 130.6 (s), 130.2 (s), 128.8 (s), 128.6 (s), 128.5 (s), 128.5 (s), 127.7 (s), 119.4 (m), 118.9 (m), 38.0 (m), 35.5 (s), 31.7 (s), 26.8 (bs) (complexity of spectrum due to ^{31}P−^{13}C coupling). ^{31}P NMR{^{1}H} (CD_2Cl_2, 300 MHz): δ 23.3. MALDI-MS: observed $C_{47}H_{48}O_2P_2PdCl$ (complex-Cl); theoretical 829.1907 (26.6%), 830.1922 (64.9%), 831.1915 (100.0%), 832.1927 (60.2%), 833.1907 (99.7%), 834.1935(45.4%), 835.1913 (57.5%), 836.1938 (25.7%), 837.1923 (14.9%); found 829.2071 (35.8%), 830.2068 (76.1%), 831.2242 (100.0%), 832.1912 (70.5%), 833.2227 (97.3%), 834.2245 (51.2%), 835.1700 (59.4%), 836.2003 (25.6%), 837.1684 (5.5%).

Preparation of Cyclooctatetradienide Solution (0.30 M). This preparation was the same as that used by Katz and co-workers.[12] THF (16 mL) was added to a flame-dried three-neck 25 mL round-bottom flask under argon and cooled to −78 °C. Lithium granules (76 mg, 11 mmol, washed with hexanes to remove mineral oil) were added under a positive flow of argon. Cyclooctatetraene (0.54 mL, 4.8 mmol) was then added via syringe. The mixture was stirred overnight while warming to room temperature to form a green-blue solution that could be stirred at room temperature until use. Best results were obtained by using the solution the same day, but it can be stored for up to 4 days with minimal decomposition.

Preparation of (4,7-Di-*tert*-butylXantphos)Pd(cyclooctatetraene) (4). Inside of a glovebox under nitrogen atmosphere, $PdCl_2$-(4,7-di-*tert*-butylXantphos) (170 mg, 0.20 mmol) was weighed into a 25 mL round-bottom flask equipped with a stirbar. The flask was sealed with a rubber septum and further sealed with black electrical tape. The flask was removed from the glovebox, and THF (8.0 mL) was added to form a yellow slurry. The slurry was degassed by three freeze/pump/thaw cycles and finally cooled to −78 °C. Cyclooctatetradienide (0.70 mL of the 0.30 M solution in THF, 0.20 mmol) was added dropwise over 5 min and then allowed to stir for 30 min to form a green slurry. Cannula transferring a portion of this solution to a flame-dried septum-sealed NMR tube under argon allowed for ^{31}P NMR analysis. Decomposition will begin to occur at room temperature, and this complex was not isolable. ^{31}P NMR{^{1}H} (THF, 300 MHz): δ 11.384 (s).

Preparation of (4,7-Di-*tert*-butylXantphos)Pd(dba) (5). Dibenzylideneacetone (280 mg, 1.2 mmol) was weighed into a 25 mL round-bottom flask and evacuated/backfilled with argon three times. The solid was dissolved in THF (5.0 mL), and the solution was then subjected to three freeze/pump/thaw cycles. While still cold, it was slowly cannula transferred to the (4,7-di-*tert*-butylXantphos)-Pd(cyclooctatetraene) solution prepared above. This mixture was stirred for 30 min while warming to room temperature to form a red-yellow solution. All attempts to isolate this complex led to decomposition. However, ^{31}P NMR analysis prior to isolation attempts revealed the species previously identified in precatalyst solutions (see Figure 8). In solution before attempted isolation: ^{31}P NMR{^{1}H} (THF, 300 MHz): δ 12.3 (d, ^2J(P,P) = 29.1 Hz), 9.82 (d, ^2J(P,P) = 29.4 Hz).

Preparation of Pd(4,7-di-*tert*-butylXantphos)$_2$ (6). 4,7-Di-*tert*-butylXantphos (830 mg, 1.2 mmol) was weighed into a 25 mL round-bottom flask and evacuated/backfilled with argon three times. The solid was dissolved in THF (5.0 mL) and then subjected to three freeze/pump/thaw cycles. While still cold, it was slowly cannula transferred to the (4,7-di-*tert*-butylXantphos)Pd(cyclooctatetraene) solution prepared above. This mixture was allowed to stir for 30 min while warming to room temperature to form a yellow solution. This yellow solution was taken into the glovebox and filtered. The resulting solution was concentrated, dissolved in benzene, filtered, and finally layered with ether. Bright yellow crystals formed, which were suitable for X-ray analysis (140 mg, 48%). Mp: 162 °C dec. IR (KBr): 3053, 2964, 2905, 2867, 2280,

1585, 1477, 1426, 1398, 1361, 1284, 1256, 1240, 742, 696 cm^{-1}. ^1H NMR (C_6D_6, 300 MHz): δ 7.05 (m, 48H), 1.78 (m, 12), 1.20 (m, 36H). ^{13}C NMR (C_6D_6, 500 MHz): δ 154.4 (bs), 153.7 (bs), 145.3 (m), 141.7 (m), 139.7 (bs), 137.4 (bs), 135.0 (s), 133.9 (s), 132.7 (m), 131.2 (bs), 124.6 (m), 123.6 (m), 121.0 (m), 36.8 (s), 35.3, (m), 33.0 (s), 32.2 (m), 22.9 (bs). ^{31}P NMR $\{^1H\}$ (C_6D_6, 300 MHz): δ 3.70 (m), 1.58 (m). Anal. Calcd for $C_{94}H_{96}O_2P_4Pd$: C, 75.87; H, 6.50. Found: C, 75.97; H, 6.48.

Preparation of Pd(Xantphos)$_2$. Xantphos (579 mg, 1.00 mmol) and $Pd_2(dba)_3$ (229 mg, 0.250 mmol) were weighed into a flame-dried 500 mL round-bottom flask and evacuated/backfilled with argon three times. Toluene (300 mL) was added, and the solution was stirred for 4 h. The solution was then filtered with a cannula filter into another flame-dried round-bottom flask under argon to remove insoluble matter. This solution was concentrated slightly and allowed to rest overnight so that any extra palladium black would settle. The resulting solution was filtered again and finally concentrated to dryness. At this point, the yellow solid was stirred in toluene (100 mL) overnight to remove dibenzylidene acetone and excess Xantphos. The remaining yellow solid was isolated by filtration and is sparingly soluble in all common organic solvents. The identity of the species was confirmed to be Pd(Xantphos)$_2$ by use of MALDI-TOF-MS analysis. IR (KBr): 2924, 2854, 1461, 1398, 1377, 1222 cm^{-1}. MALDI-MS: calcd for $C_{78}H_{64}O_2P_4Pd$: theoretical 1260.2894 (22.9%), 1261.2909 (63.4%), 1262.2911 (100.0%), 1263.2907 (64.6%), 1264.2914 (77.2%), 1265.2933 (47.5%), 1266.2931 (35.5%), 1267.2949 (25.1%); Found 1260.3405 (24.0%), 1261.3285 (67.4%), 1262.3166 (100.0%), 1263.3162 (73.2%), 1264.3300 (79.3%), 1265.3424 (47.5%), 1266.3491 (35.5%), 1267.3104 (25.1%). Anal. Calcd for $C_{78}H_{64}O_2P_4Pd$: C, 74.14; H, 5.10. Found: C, 74.44; H, 4.97. Mp: 164 °C dec.

Acknowledgment. Support has been provided by the National Institutes of Health (GM 58160), the American Chemical Society (Organic Division Fellowship to E.R.S., sponsored by Albany Molecular Research), Merck, and Novartis.

Supporting Information Available: Tables of X-ray crystallographic data, atomic coordinates, bond lengths and bond angles, and anisotropic thermal parameters for Pd(4,7-di-*tert*-butylXantphos)$_2$ (PDF and CIF files). This material is available free of charge via the Internet at http://pubs.acs.org.

OM050715G